



Influence of Reservoir Bottom Inclination on Seismic Responses of Dam-Reservoir-Foundation Coupled Systems

Santosh Kumar Das^{1)*}, Kalyan Kumar Mandal¹⁾, Arup Guha Neyogi¹⁾

¹⁾ Department of Civil Engineering, Jadavpur University, Kolkata-700032, India.

* Corresponding Author. E-Mail: santoshatju@gmail.com

ARTICLE INFO

Article History:

Received: 2/5/2025

Accepted: 13/10/2025

ABSTRACT

In this study, seismic responses of dam-reservoir-foundation coupled systems have been determined with inclined reservoir bed. The bed slope of the reservoir changes due to scouring or siltation and may affect the responses of the coupled system. In the present study, the variation of hydrodynamic pressure adjacent to the gravity dam and stresses at the heel of the dam have been observed for the change of bed slope of the reservoir in anti-clockwise and clockwise directions by applying seismic excitation including fluid-structure and soil-structure interaction. The stresses of foundation near the heel of the dam have been observed for earthquake excitation. The geometry of the coupled system is discretized using finite element and dynamic analysis of the system carried out by the direct coupling approach. Significant changes have been observed in seismic responses of the dam, reservoir and foundation for the variation of reservoir bed slope.

Keywords: Dam-reservoir-foundation system, Earthquake excitation, Hydrodynamic pressure, Direct coupling approach, Inclined reservoir base.

INTRODUCTION

Hydrodynamic pressure originates on the face of concrete of gravity dam due to earthquake. The effect of foundation also influences the responses of gravity dam. Soil-structure and fluid-structure interaction provides actual information about the responses of the gravity dam during earthquake. Bed slope of the reservoir and bottom absorption effect of the reservoir are also very important for the determination of hydrodynamic effect on the gravity dam.

Zienkiewicz and Bettess (1978) introduced two approaches; i.e., Lagrangian approach and Eulerian approach, for the solution of fluid-structure coupled problems. Tsai (1992) determined the hydrodynamic pressure considering the arbitrary dam-reservoir interface. Chen and Taylor (1990) suggested a solution

to solve fluid and structure coupled problems based on FEM. Sandberg (1995) suggested an approach for treating unsymmetrical coupled domains, like fluid-structure coupled systems. Calayir et al. (1996) presented a technique to analyse the dam-reservoir problem for earthquake force. Maity and Bhattacharya (1999) proposed a truncation boundary condition to solve the dam-reservoir problem in the time domain. Gogoi and Maity (2006) suggested a non-reflecting boundary condition to evaluate the hydrodynamic pressure. Ghorbani and Khiavi (2011) employed the Galerkin technique to develop the equation for a dam-reservoir coupled system. Wang et al. (2011) proposed an FEM technique for solving a fluid-structure problem in the time domain. Abbas and Mohammad (2012) have carried out the prediction of sedimentation in a reservoir adjacent to the Mujib dam in Jordan. Mandal and Maity

(2015) determined the responses of the aged concrete dam using the degradation index. Wang et al. (2017) proposed a method for dynamic analysis of dam-reservoir-foundation systems. Eftekhari and Jafari (2018) proposed a variational approach for dynamic analysis of the fluid-structure system. Sharma et al. (2019) used space-time finite element technique for the analysis of dam-reservoir-foundation system. Mohammadnezhad et al. (2020) investigated responses of the Pine flat dam with different earthquake excitation records. Rasa et al. (2022) proposed a technique to examine the responses of dam-reservoir-foundation systems considering radiation of waves through soil and reservoir domain. Zeyad (2022) determined the characteristic of monthly inflow of Wala dam and established the relationship between inflow and outflow. Xavier (2023) carried out the optimization of storage reservoir using neural network. Young and Louis (2023) developed a deep learning-based surrogate model for the prediction of and the robust optimization of fractured reservoir system.

Very little work has been found on the dam-reservoir-foundation problem considering the effect of the inclined reservoir bed using direct coupling approach. In the present study, hydrodynamic pressure in the reservoir and responses of gravity dam and foundation have been observed considering inclined reservoir bed applying earthquake excitation. Anti-clockwise slope of the reservoir bed is assumed as a positive slope of the reservoir bottom and clockwise slope of the reservoir bed with respect to the horizontal surface is assumed as a negative slope of the reservoir bottom. Fluid-structure and soil-structure interaction has been considered concurrently. Fluid is considered compressible and non-viscous. The bottom of the reservoir is assumed as absorptive and the effect of surface wave is neglected. Appropriate truncation boundary condition is applied at the truncation face of the reservoir and foundation domain. Two-dimensional geometry of dam-reservoir-foundation system has been discretized using the eight node isoparametric element. Earthquake excitation has been applied to study the responses of the dam, reservoir and foundation. The dynamic equilibrium equation is applied using Newmark's integration technique.

Theoretical Formulation

The dynamic equation for the dam subjected to some

external force is expressed as:

$$[M_d]\{\ddot{u}_d\} + [C_d]\{\dot{u}_d\} + [K_d]\{u_d\} = \{F_d\} \quad (1)$$

Here, $[M_d]$, $[C_d]$ and $[K_d]$ present the mass matrix, damping matrix and stiffness matrix of the dam. $\{\ddot{u}_d\}$, $\{\dot{u}_d\}$ and $\{u\}$ present the acceleration vector, velocity vector and displacement vector of the nodes. $\{F_d\}$ presents the force vector of the nodes. The stiffness matrix can be calculated as:

$$[K_d] = \iint [B]^T [D] [B] |J| d\xi d\eta \quad (2)$$

where $[B]$ denotes the strain displacement matrix. $[D]$ denotes the elasticity matrix. J denotes the Jacobian matrix. The mass matrix of the structure can be calculated as:

$$[M_d] = \int [N]^T \rho [N] d\xi d\eta \quad (3)$$

Here, ρ denotes the mass density of the dam and N denotes the shape function of the am. The Rayleigh damping model has been used for the structure and can be written as:

$$[C_d] = a'[M_d] + b'[K_d] \quad (4)$$

a' and b' are constants. a' and b' may be correlated by the expression:

$$\xi' = \frac{1}{2} \left(a' \omega + \frac{b'}{\omega} \right) \quad (5)$$

a' and b' may be determined by Eq. 6 a and Eq. 6 b.

$$a' = \frac{2(\xi_2' \omega_2 - \xi_1' \omega_1)}{(\omega_2^2 - \omega_1^2)} \quad (6a)$$

$$b' = \frac{2\omega_1 \omega_2 (\xi_2' \omega_1 - \xi_1' \omega_2)}{(\omega_2^2 - \omega_1^2)} \quad (6b)$$

Now, the equation for compressible fluid can be obtained as:

$$\nabla^2 p(x, y, t) = \frac{1}{c^2} \ddot{p}(x, y, t) \quad (7)$$

Here, ∇^2 is a two-dimensional Laplacian operator. The fluid has been considered as compressible and non-viscous. The fluid domain (Fig. 1) has been discretized

by a two-dimensional eight-node isoparametric element.

At the top of the reservoir (surface I), the following equation should be satisfied when the effect of surface wave is considered:

$$\frac{1}{g} \ddot{p} + \frac{\partial p}{\partial y} = 0 \quad (8)$$

At the interfacial surface of the dam-reservoir (surface II), the following condition has to be satisfied.

$$\frac{\partial p}{\partial n}(0, y, t) = \rho_f a e^{i\omega t} \quad (9)$$

Here, $a e^{i\omega t}$ is the acceleration, ω is the angular frequency, $i = \sqrt{-1}$. ρ_f is defined as the mass density of the liquid.

At the bottom of the fluid (surface III), the following condition has to be satisfied. Here, the absorption of energy waves has been assumed.

$$\frac{\partial p}{\partial n}(x, 0, t) = i\omega q \dot{p}(x, 0, t) \quad (10)$$

Here, $i = \sqrt{-1}$

$$q = \frac{1}{c} \left(\frac{1-\alpha}{1+\alpha} \right) \quad (11)$$

α is the reflection coefficient of the reservoir bottom.

At the truncated face (surface IV) of the reservoir, the boundary condition can be written as:

$$\frac{\partial p}{\partial n} = \left(\xi_m - \frac{1}{c} \right) \dot{p} \quad (12)$$

ξ_m is considered according to what has been suggested by I. Gogoi and D. Maity (2006).

$$\xi_m = - \frac{i \sum_{m=1}^{\infty} \frac{\lambda_m^2 I_m}{\beta_m} e^{(-k_m x)} (\psi_m)}{\Omega c \sum_{m=1}^{\infty} \frac{\lambda_m^2 I_m}{\beta_m k_m} e^{(-k_m x)} (\psi_m)} \quad (13)$$

Pressure is considered as a nodal unknown of the reservoir medium. Now, implementing the Galerkin approach, Eq. (7) can be discretized as:

$$\int_{\Omega} N_{rj} \left[\nabla^2 \sum N_{ri} p_i - \frac{1}{c^2} \sum N_{ri} \ddot{p}_i \right] d\Omega = 0 \quad (14)$$

N_{rj} denotes the interpolation functions of the fluid region domain and Ω denotes the region of fluid. Eq. (14) may be written after the application of Green's

theorem as:

$$- \int_{\Omega} \left[\frac{\partial N_{rj}}{\partial x} \sum \frac{\partial N_{ri}}{\partial x} p_i + \frac{\partial N_{rj}}{\partial y} \sum \frac{\partial N_{ri}}{\partial y} p_i \right] d\Omega - \frac{1}{c^2} \int_{\Omega} N_{rj} \sum N_{ri} d\Omega \ddot{p}_i + \int_{\Gamma} N_{rj} \sum \frac{\partial N_{rj}}{\partial n} d\Gamma p_i = 0 \quad (15)$$

Here, Γ denotes the boundary of the fluid region. The dynamic equation of the system is formed in the following manner.

$$[J]\{\ddot{p}\} + [A]\dot{p} + [H]\{p\} = \{F_r\} \quad (16)$$

Here,

$$[J] = [\bar{J}] + \frac{1}{g} [R_f] \quad (17)$$

$$[A] = \frac{1}{c} [R_t] \quad (18)$$

$$[H] = [\bar{H}] + \zeta_m [R_t] - i\omega q [R_{fb}] \quad (19)$$

$$\{F_r\} = -\rho_f [R_{fs}] \{a\} \quad (20)$$

Here,

$$[R_f] = \sum \int_{\Gamma_f} [N_r]^T [N_r] d\Gamma \quad (21)$$

$$[R_t] = \sum \int_{\Gamma_t} [N_r]^T [N_r] d\Gamma \quad (22)$$

$$[R_{fb}] = \sum \int_{\Gamma_{fb}} [N_r]^T [N_r] d\Gamma \quad (23)$$

$$[R_{fs}] = \sum \int_{\Gamma_{fs}} [N_r]^T [T] [N_d] d\Gamma \quad (24)$$

The subscripts f, fs, fb and t denote the top of the fluid region, the dam-reservoir interfacial zone, the reservoir bottom and the truncated face, respectively.

The soil foundation domain has been discretized using an eight-node isoparametric element. The well-known viscous boundary condition (Kontoe, 2009) has been applied at the truncated face of the soil in the present work.

In two-dimensional modeling, the absorbing boundary condition can be formulated from the following equations.

$$\sigma(s) + \rho c_p \dot{u}_{sl}(s) = 0 \quad (25a)$$

$$\tau(s) + \rho c_s \dot{v}_{sl}(s) = 0 \quad (25b)$$

Here, σ and τ denote normal and shear stress at the truncation surface of the soil medium. The normal and tangential damping coefficients c_n and c_t can be

expressed as follows:

$$c_n = A_1 \rho c_p \quad (26)$$

$$c_t = A_2 \rho c_s \quad (27)$$

The coefficients c_s and c_p in two mutually orthogonal directions can be expressed as:

$$c_s = \sqrt{\frac{G}{\rho}} \quad (28)$$

$$c_p = \sqrt{\frac{E(1-\nu)}{(1+\nu)(1-2\nu)\rho}} \quad (29)$$

G is the shear modulus and can be expressed as:

$$G = \frac{1}{2(1+\nu)} \quad (30)$$

For an isotropic medium, A_1 and A_2 become as follows (Kontoe, 2009). Here, s can be expressed as shown below.

$$A_1 = \frac{8}{15\pi} (5 + 2s - 2s^2) \quad (31)$$

$$A_2 = \frac{8}{15\pi} (3 + 2s) \quad (32)$$

$$s = \sqrt{\frac{(1-2\nu)}{2(1+\nu)}} \quad (33)$$

The dam, reservoir and soil foundation systems are coupled using the direct coupling approach. The dynamic equation has been solved using Newmark's method. The discrete equation of the dam considering damping may be written as:

$$\begin{bmatrix} J & Q_d^T & Q_c^T & 0 \\ 0 & M_{dd} & M_{dc} & 0 \\ 0 & M_{cd} & M_{cc} & M_{cf} \\ 0 & 0 & M_{fc} & M_{ff} \end{bmatrix} \begin{Bmatrix} \dot{P} \\ \dot{U}_d \\ \dot{U}_c \\ \dot{U}_f \end{Bmatrix} + \begin{bmatrix} A & 0 & 0 & 0 \\ 0 & C_{dd} & C_{dc} & 0 \\ 0 & C_{cd} & C_{cc} & C_{cf} \\ 0 & 0 & C_{fc} & C_{ff} \end{bmatrix} \begin{Bmatrix} \dot{P} \\ \dot{U}_d \\ \dot{U}_c \\ \dot{U}_f \end{Bmatrix} + \begin{bmatrix} H & 0 & 0 & 0 \\ -Q_d & K_{dd} & K_{dc} & 0 \\ 0 & K_{cd} & K_{cc} & K_{cf} \\ 0 & 0 & K_{fc} & K_{ff} \end{bmatrix} \begin{Bmatrix} P \\ U_d \\ U_c \\ U_f \end{Bmatrix} = \begin{bmatrix} J & Q_d^T & Q_c^T & 0 \\ 0 & M_{dd} & M_{dc} & 0 \\ 0 & M_{cd} & M_{cc} & M_{cf} \\ 0 & 0 & M_{fc} & M_{ff} \end{bmatrix} \begin{Bmatrix} F_r \\ \ddot{U}_d^g \\ \ddot{U}_c^g \\ \ddot{U}_f^g \end{Bmatrix} \quad (38)$$

Here, the subscript 'd' indicates the nodes within the dam and 'f' denotes the nodes of foundation. 'c' denotes the nodes along the dam-foundation interface. \ddot{U}_g presents the ground acceleration. Added motion approach has been used in Eq. (40). The coupling matrix is $\varrho = [Q_d] [Q_c]^T$, matrix $[Q_d]$ is related to the body of the dam and matrix $[Q_c]$ is related to the common nodes at

$$M_d \ddot{u}_d + C_d \dot{u}_d + K_d u_d - Q_p - M_d \ddot{u}_g = 0 \quad (34)$$

$[Q]$ is the coupling term that originated for acceleration and pressure at the fluid-structure interface.

$$\int_{\Gamma_{dr}} N_{dr}^T n p d\Gamma = \left(\int_{\Gamma_{dr}} N_{dr}^T n N_{dr} d\Gamma \right) p = Qp \quad (35)$$

Here, n denotes the direction vector at the dam-reservoir interface and N_{dr} is one-dimension interpolation function along the fluid-structure boundary. The equation of the fluid domain can be expressed as:

$$J \ddot{p} + A \dot{p} + H p - Q^T \ddot{u}_d - F_r = 0 \quad (36)$$

Eq. (34) and Eq. (36) can be written in matrix form, which expresses the coupled equation of the dam and reservoir as:

$$\begin{bmatrix} J & Q^T \\ 0 & M_d \end{bmatrix} \begin{Bmatrix} \ddot{p} \\ \ddot{u}_d \end{Bmatrix} + \begin{bmatrix} A & 0 \\ 0 & C_d \end{bmatrix} \begin{Bmatrix} \dot{p} \\ \dot{u}_d \end{Bmatrix} + \begin{bmatrix} H & 0 \\ -Q & K_d \end{bmatrix} \begin{Bmatrix} p \\ u_d \end{Bmatrix} = \begin{Bmatrix} F_r \\ M_d \ddot{u}_g \end{Bmatrix} \quad (37)$$

The equations for a dam-reservoir-foundation coupled problem may be accounted for; thus,

the dam-foundation interface. The absolute response of the coupled system can be expressed by a combination of free field response and added part responses and can be stated as:

$$M_{cc} = M_c^d + M_c^f, C_{cc} = C_c^d + C_c^f \text{ and } K_{cc} = K_c^d + K_c^f \quad (39)$$

$$\begin{pmatrix} \ddot{P} \\ \ddot{U}_d \\ \ddot{U}_c \\ \ddot{U}_f \end{pmatrix} = \begin{pmatrix} \ddot{P}^{ff} \\ \ddot{u}_d^{ff} \\ \ddot{u}_c^{ff} \\ \ddot{u}_f^{ff} \end{pmatrix} + \begin{pmatrix} \ddot{P}^a \\ \ddot{u}_d^a \\ \ddot{u}_c^a \\ \ddot{u}_f^a \end{pmatrix}, \quad \begin{pmatrix} \dot{P} \\ \dot{U}_d \\ \dot{U}_c \\ \dot{U}_f \end{pmatrix} = \begin{pmatrix} \dot{P}^{ff} \\ \dot{u}_d^{ff} \\ \dot{u}_c^{ff} \\ \dot{u}_f^{ff} \end{pmatrix} + \begin{pmatrix} \dot{P}^a \\ \dot{u}_d^a \\ \dot{u}_c^a \\ \dot{u}_f^a \end{pmatrix}, \quad \text{and} \quad \begin{pmatrix} P \\ U_d \\ U_c \\ U_f \end{pmatrix} = \begin{pmatrix} P^{ff} \\ u_d^{ff} \\ u_c^{ff} \\ u_f^{ff} \end{pmatrix} + \begin{pmatrix} P^a \\ u_d^a \\ u_c^a \\ u_f^a \end{pmatrix} \quad (40)$$

Here, the superscript 'ff' stands for free field response and 'a' denotes added part response. Putting

Eq. (41) in Eq. (39), we can get:

$$\begin{bmatrix} J & Q_d^T & Q_d^T & 0 \\ 0 & M_{dd} & M_{dc} & 0 \\ 0 & M_{cd} & M_{cc} & M_{cf} \\ 0 & 0 & M_{fc} & M_{ff} \end{bmatrix} \begin{pmatrix} \ddot{P}^a \\ \ddot{u}_d^a \\ \ddot{u}_c^a \\ \ddot{u}_f^a \end{pmatrix} + \begin{bmatrix} A & 0 & 0 & 0 \\ 0 & C_{dd} & C_{dc} & 0 \\ 0 & C_{cd} & C_{cc} & C_{cf} \\ 0 & 0 & C_{fc} & C_{ff} \end{bmatrix} \begin{pmatrix} \dot{P}^a \\ \dot{u}_d^a \\ \dot{u}_c^a \\ \dot{u}_f^a \end{pmatrix} + \begin{bmatrix} H \\ -[Q_d] \\ [Q_c] \\ 0 \end{bmatrix} \begin{bmatrix} 0 & 0 & 0 \\ K_{dd} & K_{dc} & 0 \\ K_{cd} & K_{cc} & K_{cf} \\ 0 & K_{fc} & K_{ff} \end{bmatrix} \begin{pmatrix} P^a \\ u_d^a \\ u_c^a \\ u_f^a \end{pmatrix} = R + F \quad (41)$$

Here,

$$R = - \begin{bmatrix} J & Q_d^T & Q_d^T & 0 \\ 0 & M_{dd} & M_{dc} & 0 \\ 0 & M_{cd} & M_{cc} & M_{cf} \\ 0 & 0 & M_{fc} & M_{ff} \end{bmatrix} \begin{pmatrix} \ddot{P}^{ff} \\ \ddot{u}_d^{ff} \\ \ddot{u}_c^{ff} \\ \ddot{u}_f^{ff} \end{pmatrix} - \begin{bmatrix} A & 0 & 0 & 0 \\ 0 & C_{dd} & C_{dc} & 0 \\ 0 & C_{cd} & C_{cc} & C_{cf} \\ 0 & 0 & C_{fc} & C_{ff} \end{bmatrix} \begin{pmatrix} \dot{P}^{ff} \\ \dot{u}_d^{ff} \\ \dot{u}_c^{ff} \\ \dot{u}_f^{ff} \end{pmatrix} - \begin{bmatrix} H \\ -[Q_d] \\ [Q_c] \\ 0 \end{bmatrix} \begin{bmatrix} 0 & 0 & 0 \\ K_{dd} & K_{dc} & 0 \\ K_{cd} & K_{cc} & K_{cf} \\ 0 & K_{fc} & K_{ff} \end{bmatrix} \begin{pmatrix} P^{ff} \\ u_d^{ff} \\ u_c^{ff} \\ u_f^{ff} \end{pmatrix} \quad (42)$$

and

$$F = - \begin{bmatrix} J & Q_d^T & Q_d^T & 0 \\ 0 & M_{dd} & M_{dc} & 0 \\ 0 & M_{cd} & M_{cc} & M_{cf} \\ 0 & 0 & M_{fc} & M_{ff} \end{bmatrix} \begin{pmatrix} F_r \\ \dot{U}_d^g \\ \dot{U}_c^g \\ \dot{U}_f^g \end{pmatrix} \quad (43)$$

Free field response is determined by analyzing the soil foundation separately. Here, the foundation has been analyzed separately. Therefore, the responses of the structure and fluid can be equated to zero. Hence, the equations can be written as:

$$\begin{pmatrix} \ddot{P} \\ \ddot{U}_d \\ \ddot{U}_c \\ \ddot{U}_f \end{pmatrix} = \begin{pmatrix} 0 \\ 0 \\ \ddot{u}_c^{ff} \\ \ddot{u}_f^{ff} \end{pmatrix} + \begin{pmatrix} \ddot{P}^a \\ \ddot{u}_d^a \\ \ddot{u}_c^a \\ \ddot{u}_f^a \end{pmatrix}, \quad \begin{pmatrix} \dot{P} \\ \dot{U}_d \\ \dot{U}_c \\ \dot{U}_f \end{pmatrix} = \begin{pmatrix} 0 \\ 0 \\ \dot{u}_c^{ff} \\ \dot{u}_f^{ff} \end{pmatrix} + \begin{pmatrix} \dot{P}^a \\ \dot{u}_d^a \\ \dot{u}_c^a \\ \dot{u}_f^a \end{pmatrix}, \quad \text{and} \quad \begin{pmatrix} P \\ U_d \\ U_c \\ U_f \end{pmatrix} = \begin{pmatrix} 0 \\ 0 \\ u_c^{ff} \\ u_f^{ff} \end{pmatrix} + \begin{pmatrix} P^a \\ u_d^a \\ u_c^a \\ u_f^a \end{pmatrix} \quad (44)$$

The free-field responses can be determined by applying seismic excitation to the foundation with the

following equation:

$$\begin{bmatrix} M_{cc} & M_{cf} \\ M_{fc} & M_{ff} \end{bmatrix} \begin{pmatrix} \ddot{u}_c^{ff} \\ \ddot{u}_f^{ff} \end{pmatrix} + \begin{bmatrix} C_{cc} & C_{cf} \\ C_{fc} & C_{ff} \end{bmatrix} \begin{pmatrix} \dot{u}_c^{ff} \\ \dot{u}_f^{ff} \end{pmatrix} + \begin{bmatrix} K_{cc} & K_{cf} \\ K_{fc} & K_{ff} \end{bmatrix} \begin{pmatrix} u_c^{ff} \\ u_f^{ff} \end{pmatrix} = - \begin{bmatrix} M_{cc} & M_{cf} \\ M_{fc} & M_{ff} \end{bmatrix} \begin{pmatrix} \dot{U}_c^g \\ \dot{U}_f^g \end{pmatrix} \quad (45)$$

After getting the free field responses, the interaction force R can be determined by using the following

expression:

$$R = - \begin{bmatrix} 0 & 0 & 0 & 0 \\ 0 & M_{dd} & M_{dc} & 0 \\ 0 & M_{cd} & M_{cc}^d & 0 \\ 0 & 0 & 0 & 0 \end{bmatrix} \begin{pmatrix} 0 \\ 0 \\ \ddot{u}_c^{ff} \\ 0 \end{pmatrix} - \begin{bmatrix} 0 & 0 & 0 & 0 \\ 0 & C_{dd} & C_{dc} & 0 \\ 0 & C_{cd} & C_{cc}^d & 0 \\ 0 & 0 & 0 & 0 \end{bmatrix} \begin{pmatrix} 0 \\ 0 \\ \dot{u}_c^{ff} \\ 0 \end{pmatrix} - \begin{bmatrix} 0 & 0 & 0 & 0 \\ 0 & K_{dd} & K_{dc} & 0 \\ 0 & K_{cd} & K_{cc}^d & 0 \\ 0 & 0 & 0 & 0 \end{bmatrix} \begin{pmatrix} 0 \\ 0 \\ u_c^{ff} \\ 0 \end{pmatrix} \quad (46)$$

For the determination of absolute responses of dam-reservoir-foundation coupled systems, the following steps are needed to be followed.

domains are calculated.

Step I: the interaction force R in Eq. (46) is determined.

Step III: Free field response and calculated added responses are needed to be summed up for absolute response of dam-reservoir-foundation coupled systems.

Step II: As per Eq. (41), the added responses of the three

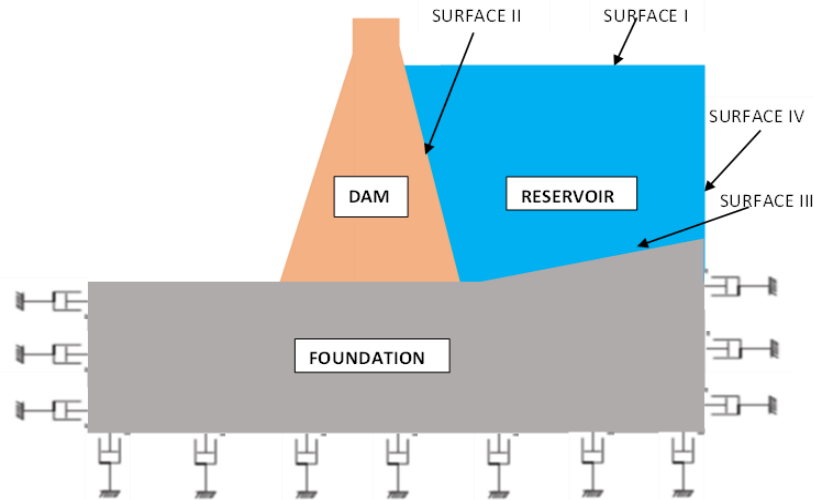


Figure 1. Geometry of dam-reservoir-foundation coupled system

Validation of Developed Algorithm

The developed algorithm is checked with the example used by Papazafeiropoulos et al. (2011). The density of water (ρ_f) is assumed as 1000kg/m^3 and velocity of sound (c) is considered to be 1440 m/s . Modulus of elasticity of the structure is considered as $3.15 \times 10^{10}\text{ N/m}^2$ and density of the gravity dam is assumed as 2400kg/m^3 . Here, the damping is taken as

5%. Modulus of elasticity of the foundation is taken as $3.15 \times 10^{10}\text{ N/m}^2$ and density is assumed to be 2400kg/m^3 . Pressure distribution at the dam face is presented in Fig. 2 by applying a sinusoidal excitation of frequency of $Tc/H_f=10$. The outcomes of the study are in conformity with those of Papazafeiropoulos et al. (2011).

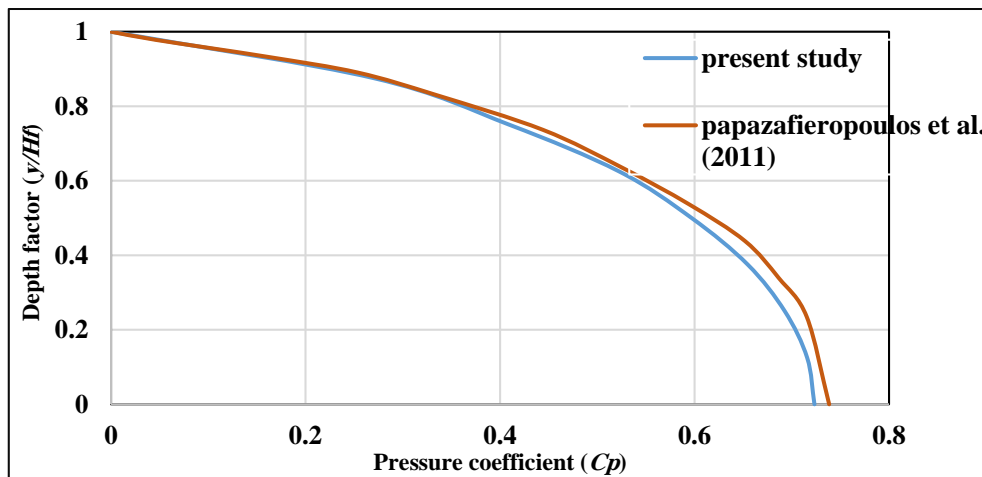


Figure 2. Hydrodynamic pressure at the face of the dam

NUMERICAL RESULTS

In the present work, changes of hydrodynamic pressure and stresses of gravity dam have been obtained by the dynamic analysis of dam-reservoir-foundation coupled system. A typical geometry of the coupled system is shown in Fig. 3. The dimensions of soil foundation (length=350 m., height =100 m.) is taken as per the reference of Mandal and Maity (2017). Height of

fluid (H_f) is taken as 103 m. Density of fluid (ρ_f) is taken as 1000 kg/m^3 and velocity of sound in water is assumed to be 1438.7 m/s . Modulus of elasticity of the dam is taken as $3.15 \times 10^{10}\text{ N/m}^2$ and density of the structure is taken as 2415.816 kg/m^3 . Poisson ratio is considered as 0.235. Modulus of elasticity of the foundation is taken as $1.75 \times 10^{10}\text{ N/m}^2$ and density is assumed as 1800kg/m^3 . Poisson ratio for soil foundation is taken as 0.2 and reflection coefficient (α) of the reservoir bottom

is taken as 0.95. Hydrodynamic pressure and stresses of the dam and foundation are observed for various

bottom slopes of the reservoir.

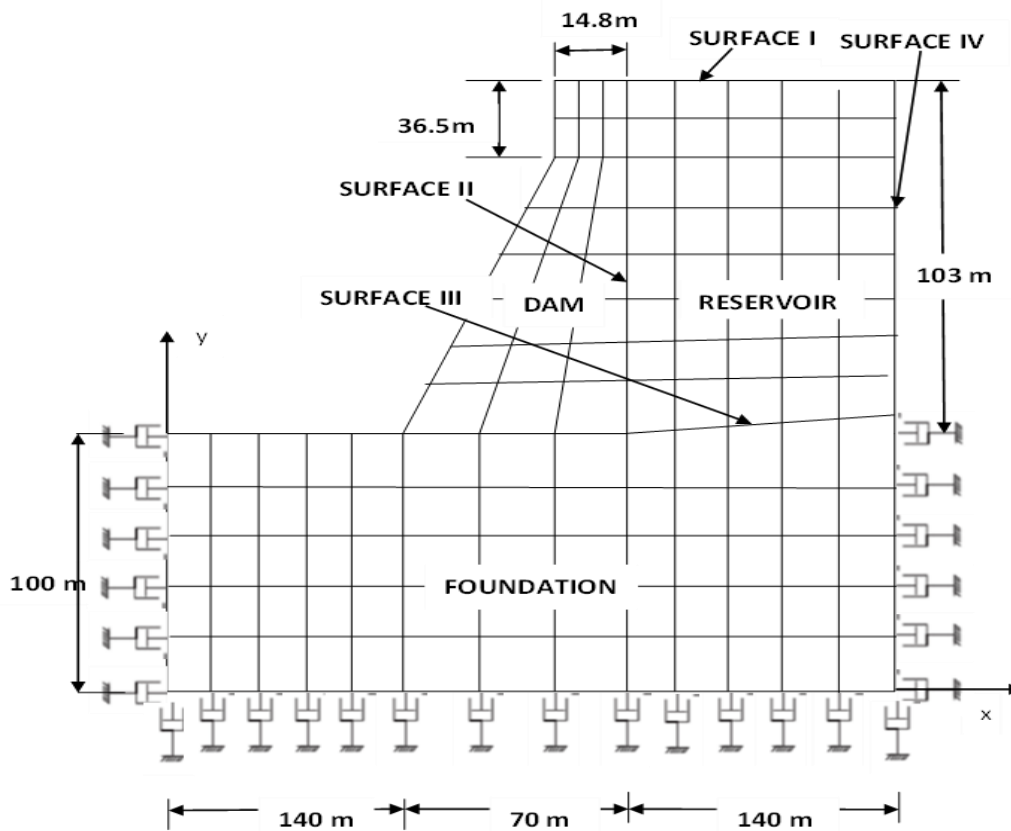


Figure 3. Typical finite element discretization of dam-reservoir-foundation coupled system

Hydrodynamic pressure at the upstream face of the dam is observed by applying seismic excitation for different slope angles of the reservoir bed considering dam-reservoir-foundation interaction. Stresses of dam and foundation are also observed for earthquake excitation. Here, the north-south component of El-Centro earthquake excitation is applied for the analysis. Fig. 4.a presents changes of pressure coefficient ($C_p = p/\rho_f a H_f$) at the dam face for positive bottom slope ($+5^\circ$, $+10^\circ$ and $+15^\circ$). Fig. 4.b presents changes of pressure coefficient (C_p) at the dam face for negative bottom slope (-5° , -10° and -15°). Fig. 5.a shows the plot of pressure coefficient (C_p) at the heel of the dam for positive bed slope. Fig. 5.b shows the plot of pressure coefficient (C_p) at the heel of the dam for negative bed slope. From these figures, it has been found that pressure rises at the heel of the dam due to increment of positive bed slope and pressure reduces at the same place for increment of negative bed slope.

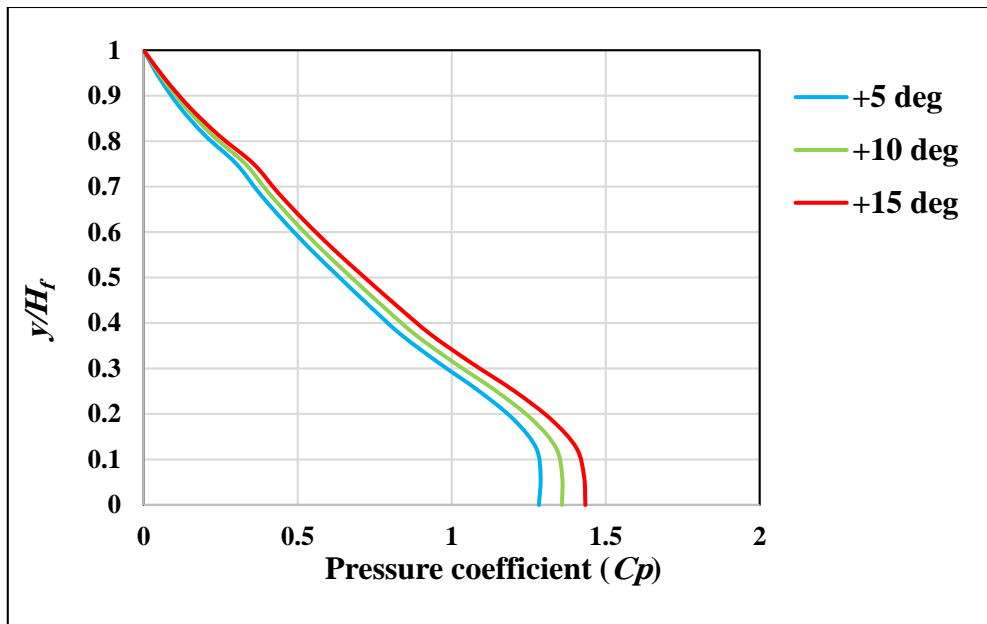
Fig. 6.a to Fig. 6.f show the velocity profile of the

reservoir for different values of bed slope of the reservoir. Hydrodynamic pressure changes due to the change in bed slope. For this reason, a difference in velocity profile of the reservoir has been seen for different values of bed slope of the reservoir. Fig 7.a and Fig. 7.b present principal stresses at the heel of the structure for positive bed slopes. Fig 8.a and Fig. 8.b present principal stresses at the heel of the structure for negative bed slopes. It has been clear that the maximum stress (major and minor) at the heel of the dam increased for increase in positive slope angles ($+5^\circ$, $+10^\circ$ and $+15^\circ$) at the base of the reservoir and the maximum stress (major and minor) at the heel of the dam decreased for increase in negative slope angles (-5° , -10° and -15°) at the base of the reservoir.

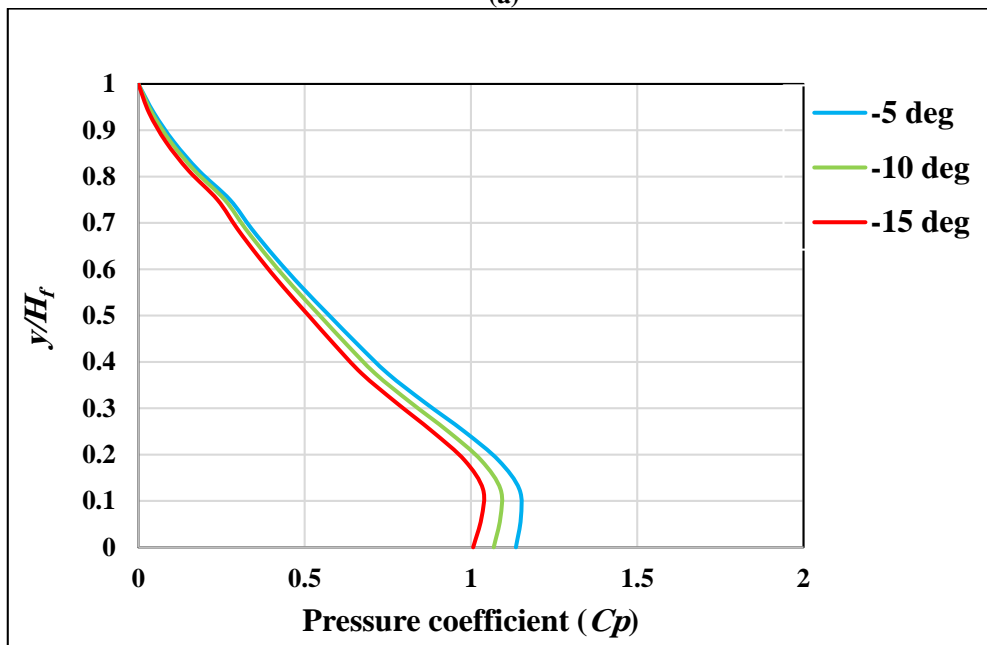
Fig. 9.a shows the plot of major principal stress and Fig. 9.b shows the plot of minor principal stress of the foundation near the heel of the dam for positive slope angles ($+5^\circ$, $+10^\circ$ and $+15^\circ$) due to earthquake excitation. Fig. 10.a shows the plot of major principal stress and Fig.

10.b shows the plot of minor principal stress of the foundation near the heel of the dam for negative slope angles (-5° , -10° and -15°). From these figures, it has been seen that the maximum stress (major and minor) of the foundation near the heel of the structure decreased with increment of positive slope angle of the reservoir bed due to earthquake excitation. It has been also seen that the maximum stress (major and minor) of the foundation near

the heel of the structure increased with increment of the negative slope angle of the reservoir bed due to earthquake excitation. Fig. 11 a. to Fig. 11.f, presented in the supplementary data file, show the contour of pressure and stresses for different bed slopes of the reservoir. These figures show that that maximum hydrodynamic pressure and maximum stress in the reservoir to occur at the heel of the structure due to earthquake excitation.

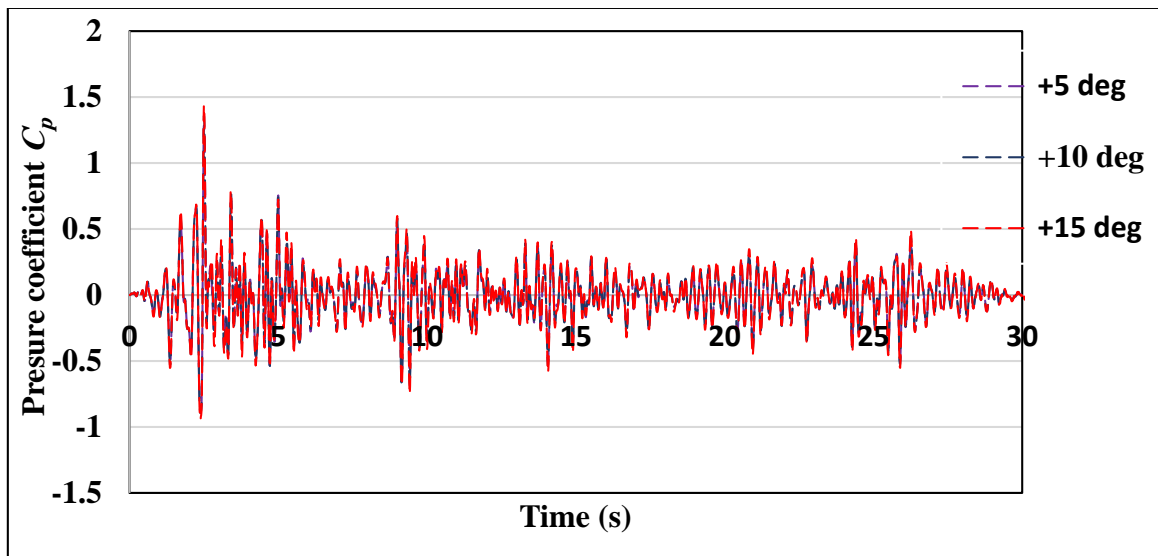


(a)

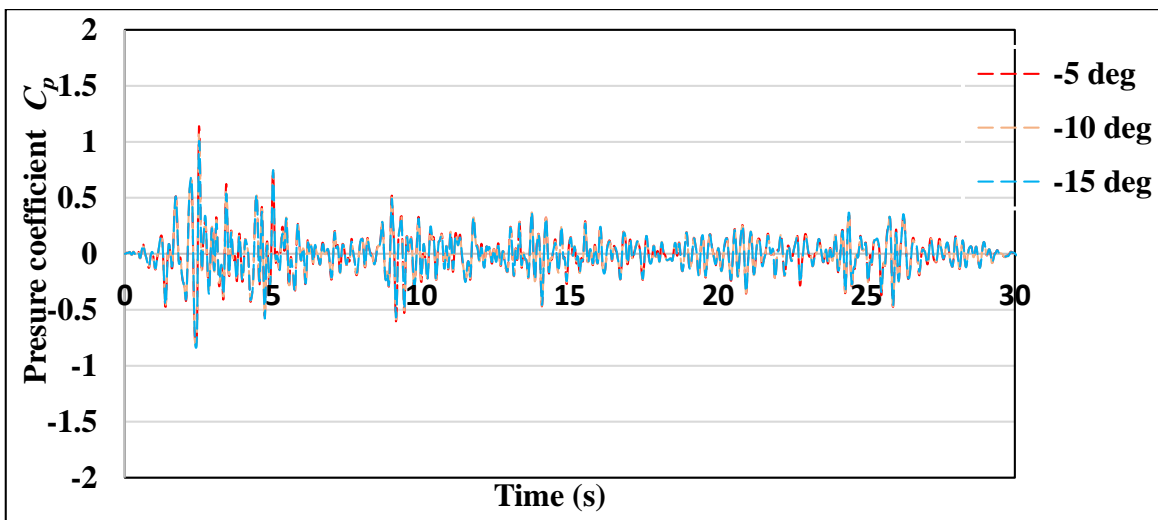


(b)

Figure 4. Pressure coefficient (C_p) at the dam face with different bottom slopes θ_b a) for positive and b) for negative slope angles due to north–south component of El-Centro earthquake



(a)



(b)

Figure 5. Time history of pressure coefficient (C_p) at the heel of the dam for different bottom slopes a) positive and b) negative slope angles for north-south component of El-Centro earthquake

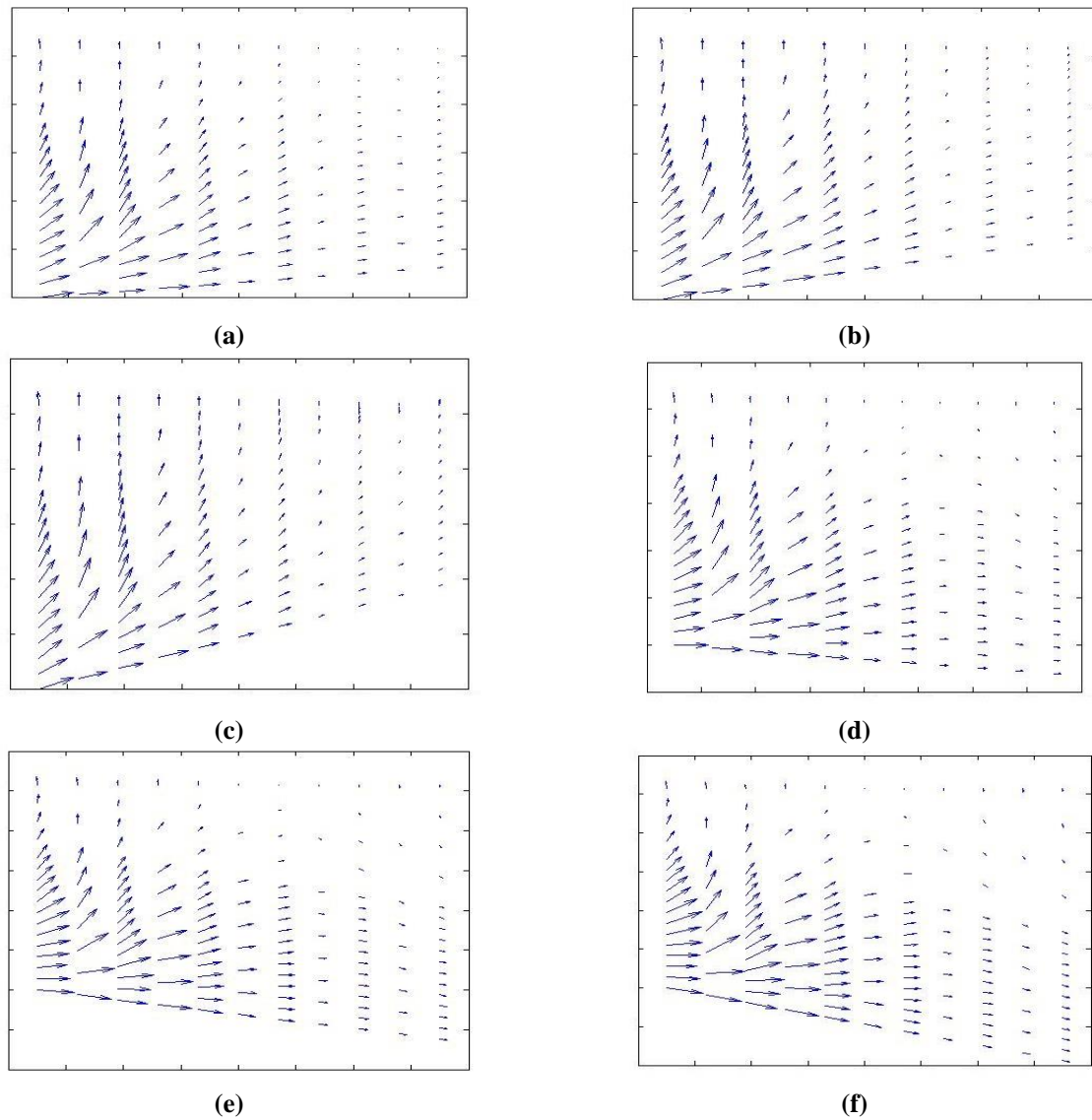


Figure 6. Velocity profile of the reservoir at 2.52 sec. for a) $\theta_b = +5^\circ$, b) $\theta_b = +10^\circ$, c) $\theta_b = +15^\circ$, d) $\theta_b = -5^\circ$, e) $\theta_b = -10^\circ$, f) $\theta_b = -15^\circ$ for north–south component of El-Centro earthquake

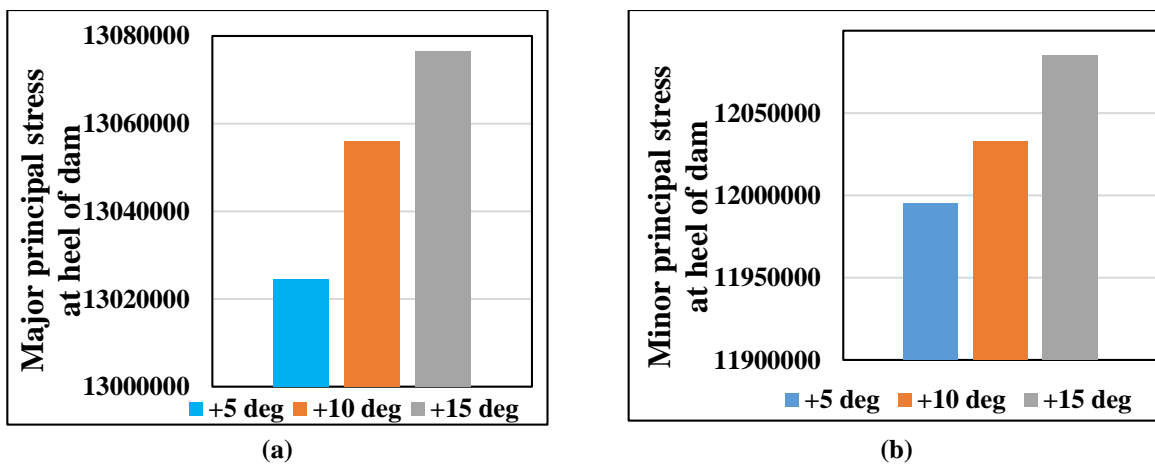


Figure 7. a) Major principal stress and b) minor principal stress at the heel of the dam for positive bed slopes of the reservoir for the north–south component of El-Centro earthquake

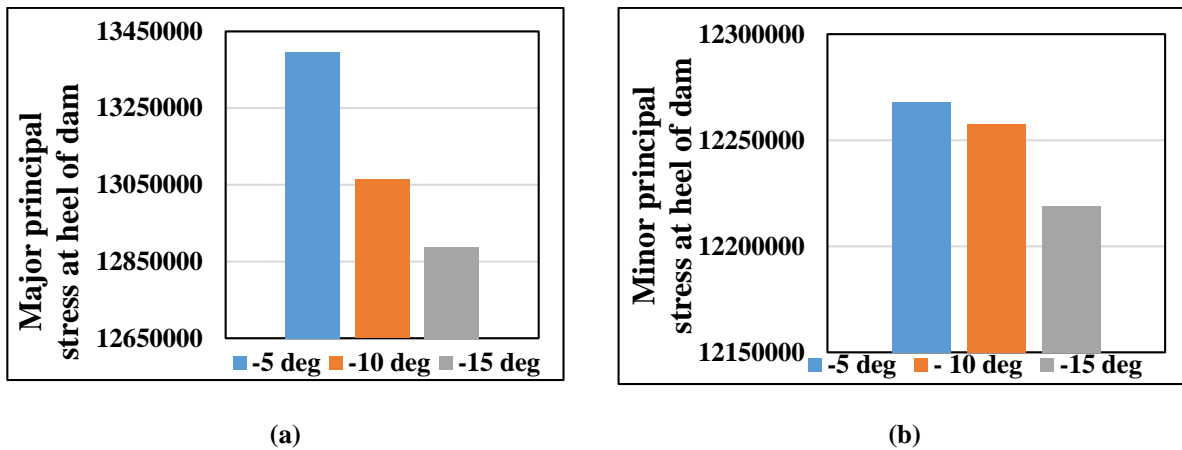


Figure 8. a) Major principal stress and b) minor principal stress at the heel of the dam for negative bed slopes of the reservoir for north–south component of El-Centro earthquake

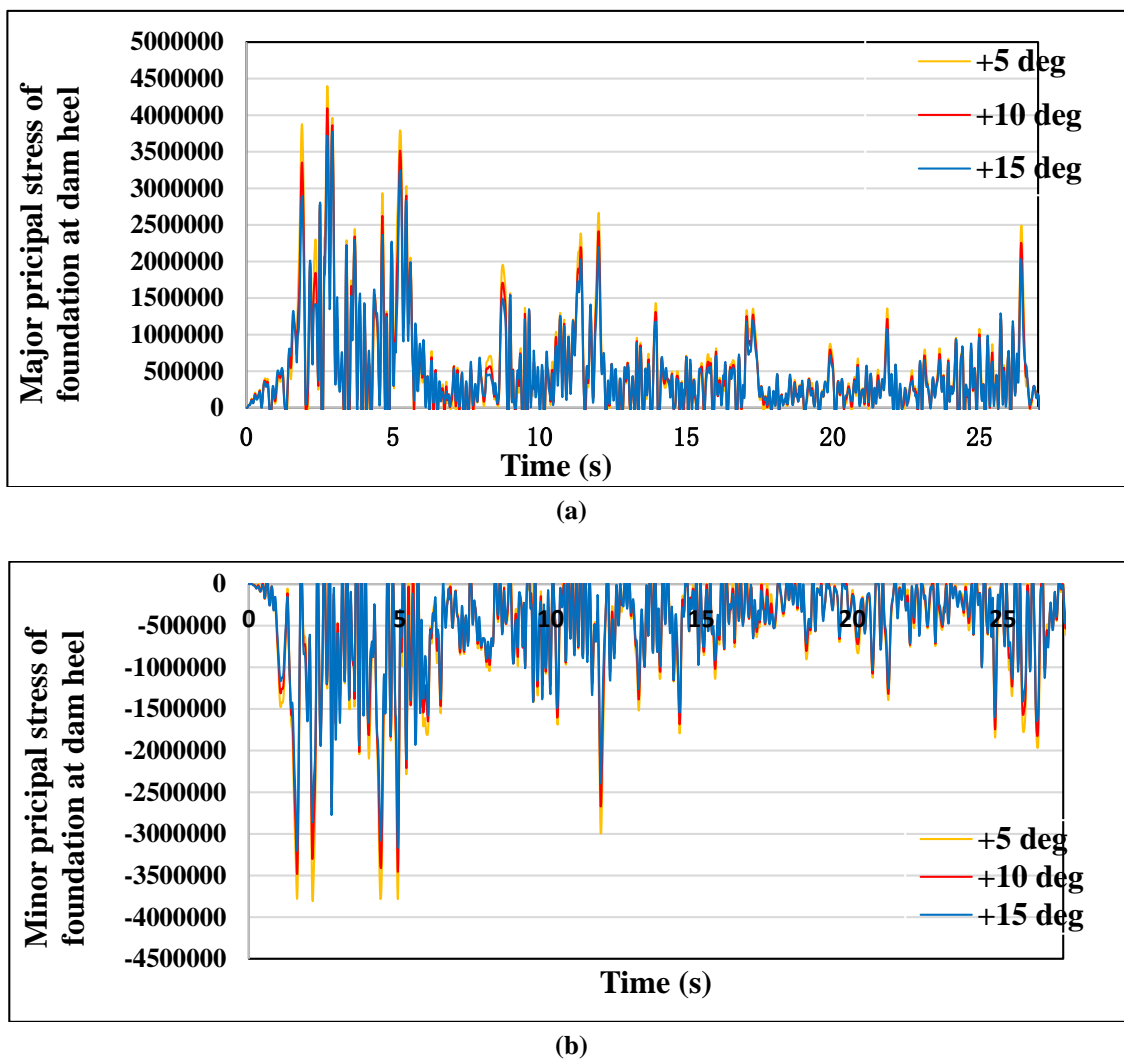


Fig. 9. Time history plot of a) major principal stress and b) minor principal stress of the foundation at the dam heel for positive bottom slopes due to north–south component of El-Centro earthquake

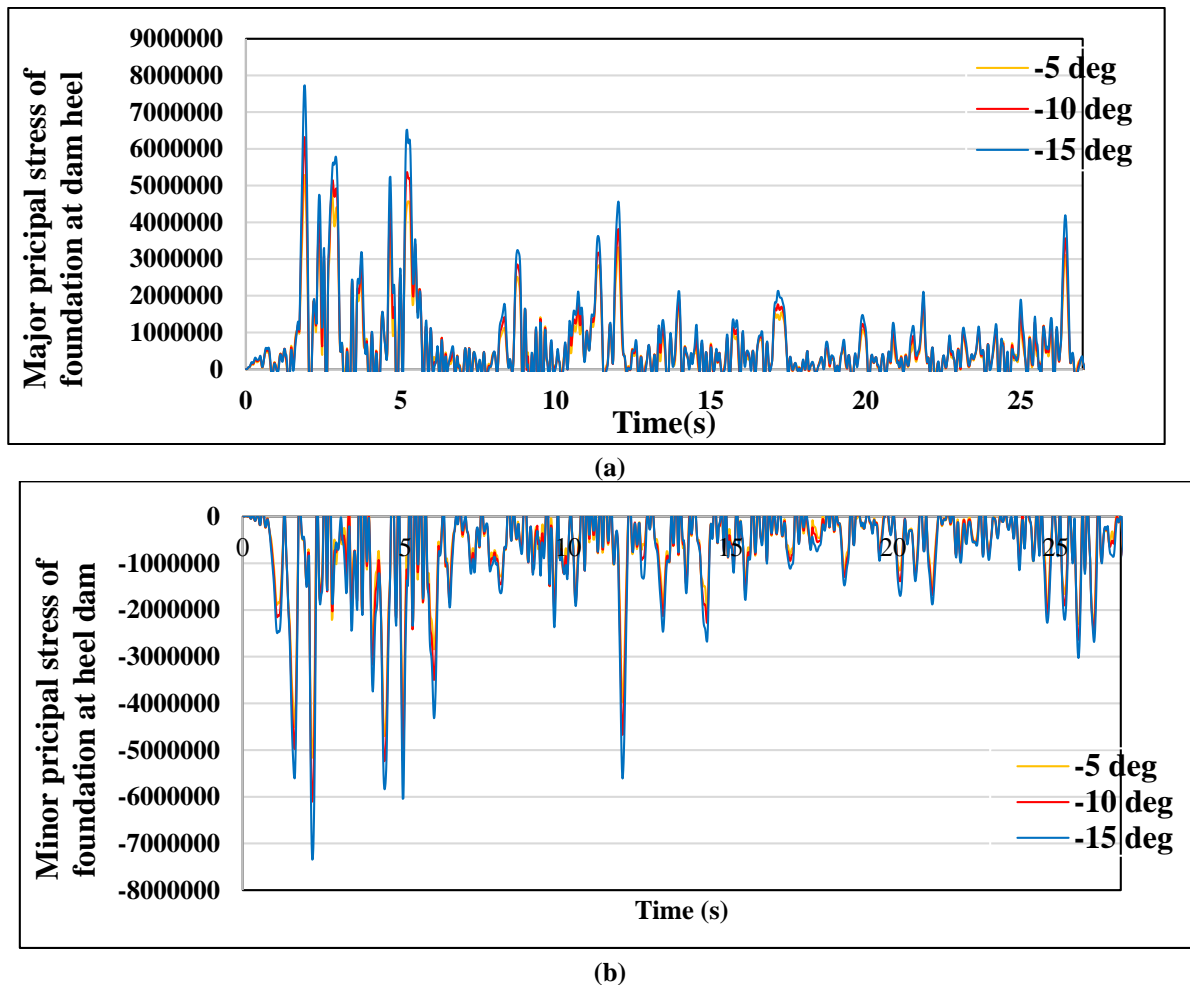


Figure 10. Time history plot of a) major principal stress and b) minor principal stress of the foundation at the dam heel for negative bottom slopes due to north-south component of El-Centro earthquake

DISCUSSION

It has been observed that hydrodynamic pressure and stresses at the heel of the dam increases for increment of positive (anti-clockwise) bed slope angle of the reservoir. Due to positive (anticlockwise) inclination, the reservoir bed reflects the wave towards the structure and amplifies the responses of the reservoir and gravity dam. This is the main reason for obtaining more pressure in the reservoir and stresses at the heel of the structure for incremental values of positive (anti-clockwise) bottom slope of the reservoir. It has been further seen that hydrodynamic pressure and stresses at the heel of the structure is decreased gradually due to increment of negative (clockwise) bed slope of the reservoir. When the reservoir bed slope is in negative (clockwise) direction, the depth of the reservoir increases as we further move away from the dam-water interface. Due to negative (clockwise) inclination, the reservoir bed

reflects the wave further away from the dam, thus reducing the responses of the reservoir and the structure.

From the present study, it has been also observed that stresses of the foundation under the heel of the structure decreased with the increase of positive (anticlockwise) bed slope of the reservoir. When the reservoir bottom slope is positive (anticlockwise), the stiffness contribution due to the foundation increases for the increase in the volume of soil foundation. As a result, stresses in the foundation under the heel of the dam reduced with the increment of positive (anti-clockwise) bed slope of the reservoir. The reverse condition occurred when the reservoir bed is inclined in a negative (clockwise) direction.

CONCLUSIONS

Based on the numerical results and the observations from the present study, specific conclusions are given below.

- The hydrodynamic pressure at the heel of the dam rises with the increment of the bed slope of the reservoir for positive (anti-clockwise) slope angles. The main reason behind that is that the reservoir bed reflects the disturbing waves towards the gravity dam for anti-clockwise slope. However, the pressure at the heel of the dam decreases with the increment of bed slope of the reservoir for negative (clockwise) slope angles. When the reservoir bed is inclined in the negative (clockwise) direction, the energy content of the disturbing forces is reflected outward in the form of waves.
- Stresses at the heel of the dam rise with the increment of slope angles of the reservoir bed for positive (anti-clockwise) slopes. However, for negative (clockwise) bed slopes, stresses at the same location decreased with the increment of bed slope.
- The stress of the foundation under the heel of the dam decreases with the increment of slope angle for positive (anti-clockwise) bed slopes. However, stress at this location increases with the increment of negative (clockwise) slope angles.

- Hydrodynamic pressure and stresses at the heel of the dam reduced due to negative (clockwise) slope of the reservoir bed. The slope of the reservoir may change due to siltation. If the bed slope is in the anticlockwise direction, then the stresses and pressure at the heel of the dam may increase. This may cause the failure of the structure. So, the removal of silt from the bottom of the reservoir by dredging with proper planning can be beneficial for the safety and stability of the dam.
- In the present work, two-dimensional analysis has been conducted. Three-dimensional analysis of the system in future research may give a clearer idea about the inclination of the reservoir bed slope.
- The findings may be established very well if the study will be conducted with different truncation boundary conditions and different absorption coefficients.

Conflict of Interests

The authors declare no conflict of interests

REFERENCES

- Abbas, Z.I., & Al-Mahamid, M.H. (2012). Predicting sedimentation at Mujib Dam reservoir in Jordan. *Jordan Journal of Civil Engineering*, 6(4), 448-463.
- Calayir, Y., Dumanoglu, A.A., & Bayraktar, A. (1996). Earthquake analysis of gravity dam-reservoir systems using the Eulerian and Lagrangian approaches. *Computers & Structures*, 59(5), 877-890.
- Chen, H.C., & Taylor, R.L. (1990). Vibration analysis of fluid-solid systems using a finite element displacement formulation. *International Journal for Numerical Methods in Engineering*, 29, 683-698.
- Eftekhari, S.A., & Jafari, A.A. (2018). A Ritz procedure for transient analysis of dam-reservoir interaction. *Iranian Journal of Science and Technology, Transactions of Civil Engineering*.
- Gogoi, I., & Maity, D. (2006). A non-reflecting boundary condition for the finite element modeling of infinite reservoir with layered sediment. *Advances in Water Resources*, 29, 1515-1527.
- Ghorbani, M.A., & Khiavi, M.P. (2011). Hydrodynamic modeling of infinite reservoir using finite element method. *International Journal of Civil, Environmental, Structural, Construction and Architectural Engineering*, 5(8), 324-328.
- Maity, D., & Bhattacharya, S.K. (1999). Time-domain analysis of infinite reservoir by finite element method using a novel far-boundary condition. *Finite Elements in Analysis and Design*, 32, 85-96.
- Mandal, K.K., & Maity, D. (2015). Seismic response of aged concrete dam considering interaction of dam and reservoir in coupled way. *Asian Journal of Civil Engineering (BHRC)*, 17(5), 571-592.
- Mandal, K.K., & Maity, D. (2017). Seismic response of a dam-reservoir-foundation coupled system with long-term ageing of dam. *Dam Engineering*, 27(3), 1-30.
- Mohammadnezhad, H., Saeednezhad, N., & Sotoudeh, P. (2020). The effect of earthquake frequency content and soil-structure interaction on the seismic behavior of concrete gravity dam-foundation-reservoir. *Numerical Methods in Civil Engineering*, 4(4), 1-20.
- Papazafeiropoulos, G., Tsompanakis, Y., & Psarropoulos, P.N. (2011). Dynamic interaction of concrete dam-reservoir-foundation: Analytical and numerical solutions. *Computational Methods in Applied Sciences*, 21, 455-488.
- Rasa, A.Y., Budak, A., & Duzgun, O. A. (2022). An efficient finite element model for dynamic analysis of gravity dam-reservoir-foundation interaction problems.

- Latin American Journal of Solids and Structures*, 19(6), 1-21.
- Sandberg, G. (1995). A new strategy for solving fluid-structure problems. *International Journal for Numerical Methods in Engineering*, 38, 357-370.
- Sharma, V., Fujisawa, K., & Murakami, A. (2019). Space-time finite element procedure with block-iterative algorithm for dam-reservoir-soil interaction during earthquake loading. *International Journal for Numerical Methods in Engineering*, 120, 263-282.
- Tsai, C.S. (1992). Semi-analytical solution for hydrodynamic pressures on dams with arbitrary upstream face considering water compressibility. *Computers & Structures*, 42(4), 491-502.
- Wang, X., Jin, F., Prempramote, S., & Song, C. (2011). Time-domain analysis of gravity dam-reservoir interaction using high-order doubly asymptotic open boundary. *Computers & Structures*, 89, 668-680.
- Wang, Y.Y., Li, J.Y., Ning, B.K., & Zhang, P. (2017). Seismic response analysis of reservoir water-gravity dam-foundation system. *Key Engineering Materials*, 737, 494-499.
- Xavier, W. (2023). Reservoir optimization and machine learning methods. *EURO Journal on Computational Optimization*, 11(100068), 1-13.
- Young, D.K., & Louis, J.D. (2023). Neural network surrogate for flow prediction and robust optimization in fractured reservoir systems. *Fuel*, 351(128756), 1-10.
- Zayed, T. (2022). The characteristics of the Wala Dam monthly inflow and the relationship between inflow and outflow. *Jordan Journal of Civil Engineering*, 16(3), 497-506.
- Zienkiewicz, O.C., & Bettess, P. (1978). Fluid-structure dynamic interaction and wave forces: An introduction to numerical treatment. *International Journal for Numerical Methods in Engineering*, 13, 1-16.